Journal of Cardiovascular Magnetic Resonance (2007) **9,** 741–747

ISSN: 1097-6647 print / 1532-429X online
DOI: 10.1080/10976640701544530

informa
healthcare

Transit of Blood Flow Through the Human Left Ventricle Mapped by Cardiovascular Magnetic Resonance

Ann F. Bolger, MD, FAHA,[1,2] Einar Heiberg, PhD,[2,3] Matts Karlsson, PhD,[2,4], Lars Wigström, PhD,[2,3] Jan Engvall, MD, PhD,[2,3] Andreas Sigfridsson, MSc,[2,3] Tino Ebbers, PhD,[2,3] John-Peder Escobar Kvitting, MD, PhD,[2,3] Carl Johan Carlhäll, MD, PhD,[2,3] and **Bengt Wranne, MD, PhD[2,3]**

Department of Medicine, University of California, San Francisco, California, USA[1] Center for Medical Image Science and Visualization, Linköping University,[2]; Division of Clinical Physiology, Department of Medicine and Care, Linköping University,[3] Division of Biomedical Modeling and Simulation, Department of Biomedical Engineering,[4] Linköping University, Linköping, Sweden

ABSTRACT

***Background*: The transit of blood through the beating heart is a basic aspect of cardiovascular physiology which remains incompletely studied. Quantification of the components of multidirectional flow in the normal left ventricle (LV) is lacking, making it difficult to put the changes observed with LV dysfunction and cardiac surgery into context. *Methods:* Three dimensional, three directional, time resolved magnetic resonance phase-contrast velocity mapping was performed at 1.5 Tesla in 17 normal subjects, 6 female, aged 44 $\pm$ 14 years (mean $\pm$ SD). We visualized and measured the relative volumes of LV flow components and the diastolic changes in inflowing kinetic energy (KE). Of total diastolic inflow volume, 44 $\pm$ 11% followed a direct, albeit curved route to systolic ejection (videos 1 and 2), in contrast to 11% in a subject with mildly dilated cardiomyopathy (DCM), who was included for preliminary comparison (video 3). In normals, 16 $\pm$ 8% of the KE of inflow was conserved to the end of diastole, compared with 5% in the DCM patient. Blood following the direct route lost or transferred less of its KE during diastole than blood that was retained until the next beat (1.6 $\pm$ 1.0 millijoules vs 8.2 $\pm$ 1.9 millijoules, $p < 0.05$); whereas, in the DCM patient, the reduction in KE of retained inflow was 18-fold greater than that of the blood tracing the direct route. *Conclusion:* Multidimensional flow mapping can measure the paths, compartmentalization and kinetic energy changes of blood flowing into the LV, demonstrating differences of KE loss between compartments, and potentially between the flows in normal and dilated left ventricles.**

INTRODUCTION

Inside the beating ventricle, blood cells find their path through a trabeculated cavern with rapidly changing size, shape and potentially competing flows. Computational modeling (1–4), pressure catheters (5), and two-dimensional imaging methods (6, 7) have given information on some aspects of flow within the ventricle, particularly near the valves. Other areas within the LV cavity are less well characterized. Planar imaging or methods based on unidirectional velocity measures, such as Doppler ultrasound, have not been adequate to describe, nor effectively measure the time-varying and intrinsically three dimensional characteristics of blood flow within the cavities of the heart.

Many features of normal left ventricular (LV) flow have been incorporated in a growing understanding of cardiac flow behavior (8–14). Flow streaming, vortices and core flow regions are components of the normal flow of both left and right ventricles, and functional advantages have been attributed to their distribution in normal hearts (12) and in the setting of heart failure and valve disease (15–17).

In order to provide a context for these previous observations and to address persistent questions about normal LV flow

Received 23 August 2006; accepted 12 April 2007.
Keywords: Blood Flow, Left Ventricle, Kinetic Energy
This work was supported by the Swedish Research Council and the Swedish Heart-Lung Foundation. The authors would like to acknowledge the thoughtful input of Dr. Neil Ingels.
Correspondence to:
Ann F. Bolger, MD
William Watt Kerr Professor of Clinical Medicine
Department of Medicine
University of California, San Francisco
1001 Potrero Avenue 5G1
San Francisco CA 94110
tel: 415 206 8087; fax: 415 206 5100
email: abolger@medsfgh.ucsf.edu

organization, we sought to describe the spatial distribution and components of dynamic LV flow using intrinsically three dimensional, three directional, time resolved velocity mapping. We hypothesized that visualization of the separate components of normal LV inflow would differentiate distributions among LV regions, and that it would be possible to identify a direct pathway through the LV that minimizes the loss of kinetic energy (KE) during diastole.

METHODS

Phase contrast CMR data acquisition

Three dimensional, three directional, time resolved velocity data were collected from 17 healthy volunteers between 24 to 62 years of age (Table 1), as well as a single subject with dilated cardiomyopathy (DCM). All normal subjects demonstrated normal systolic and diastolic left ventricular function by transthoracic echocardiography. All subjects gave informed consent, and the study was approved by the regional ethics committee for human research at the Faculty of Health Sciences, Linköping University, Sweden.

A 1.5 T CMR scanner (Signa Horizon, GE Healthcare, Milwaukee, Wisconsin, USA) was used with a modified 3D phase contrast pulse sequence to acquire time-resolved 3D velocity data from an axial volume encompassing the entire heart (Fig. 1a) (18). Acquisition parameters used were: repetition time (TR) = 18 ms, echo time (TE) = 6 ms, flip angle = 20°, number of excitations (NEX) = 1 and velocity encoding range (VENC) = ±60 cm/s in all three directions. Temporal phase unwrapping was applied to extend the usable velocity range (19, 20). Spatial resolution was $1 \times 4 \times 4$ mm^3 (FOV $300 \times 300 \times 112$ mm^3, matrix $256 \times 76 \times 28$) or $1 \times 3 \times 8$ mm^3 (FOV $300 \times 300 \times 128$ mm^3, matrix $256 \times 96 \times 16$) in the frequency (right-left), phase (anterior-posterior) and slice (superior-inferior) encoding directions, respectively. With the first parameter setting, only a cylindrical region of k-space was acquired, and the corners of the kykz plane were zero filled, resulting in a scan time of approximately 30 minutes with both settings. With the four velocity encoded echoes interleaved and no further k-space segmentation used, the temporal resolution was 72 ms. Every k-space line was sampled during an interval of at least 1.15 seconds. In the offline retrospective reconstruction, samples falling outside the first heart cycle were wrapped back into the first beat, which improved the temporal resolution at heart rates above 52 bpm (20). The acquired k-space data were zero filled to a matrix size of $256 \times 256 \times 32$ prior to the Fourier transform, resulting in a voxel size of $1 \times 1 \times 4$ mm in the reconstructed velocity data. Thirty two time steps were retrospectively interpolated over the cardiac cycle. The obtained velocity data were subsequently corrected for Maxwell effects based on the gradient waveforms used (21), and for eddy current effects by subtracting a linear three-dimensional function fitted to regions containing stationary tissue. Additional two-dimensional slices were acquired separately to aid in anatomical orientation. Intracardiac vortices were automatically identified with a previously described flow characterization technique (22).

Table 1. Subject characteristics

	Subject	Age (years)	Gender	Heart Rate (bpm)
Normals:	1	24	F	50
	2	49	M	51
	3	62	M	52
	4	45	M	55
	5	59	M	56
	6	25	M	57
	7	50	M	60
	8	26	M	61
	9	58	M	63
	10	54	F	63
	11	57	M	68
	12	56	M	70
	13	33	M	71
	14	57	F	72
	15	26	F	82
	16	29	F	82
	17	42	F	82
Patient:	DCM	51	M	62
Normal Subjects	Average ± SD:	44 ± 14		64.3 ± 10.8
	Range:	24 – 62	M 11/F 6	50 – 82

bpm = beats per minute, DCM = dilated cardiomyopathy, SD = standard deviation.

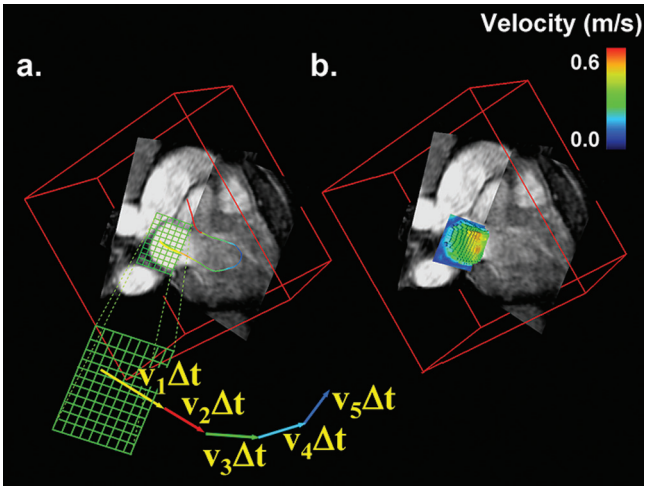

Figure 1. Three dimensional intracardiac velocity data can be visualized according to region or flow of interest. (**a**) The three-dimensional data set (red box) incorporates the cardiac structures (gray scale orientation slices). Particle trace pathlines are calculated from velocity (v) data integrated over time (t) starting from a point of interest (green emission grid). (**b**) Inflow traces are shown as they arise from the original rectangular emitter plane during their first time step. Their origins define the irregularly shaped mitral annular area.

Particle trace analysis

A particle trace is the path that an imaginary particle would take through a velocity field from a given starting point and time

(Fig. 1a) (23, 24). We calculated these trajectories by integration of the multidimensional velocity data that we acquired (20). A commercially available flow visualization package (EnSight, CEI Inc, Apex, North Carolina, USA) was used to interactively place particle trace emitters and region-of-interest (ROI) planes and to calculate and visualize the particle traces (20). Subsequent analysis of the particle trace velocity and spatial coordinates was done using customized software developed in Matlab (The MathWorks Inc., Natick, Massachusetts, USA).

Flow separation and visualization

A rectangular emitter grid was placed in the left atrium near the anatomic position of the mitral annulus at end-diastole; the emitter was sized to exceed the atrial confines in order to include all possible inflow (Fig. 1b). Four hundred particle traces were emitted from a 20 × 20 grid at each time step throughout the cardiac cycle. Inflow traces were identified by requiring that they cross a plane placed downstream at the mitral vena contracta (VC). The irregular mitral annular shape is identified by the origins of the inflow traces (Fig. 1b).

A subset of inflow traces crossed planes at both the mitral vena contracta and the left ventricular outflow tract (LVOT) within one cardiac cycle; these were considered *Direct flow*. *Retained inflow* traces crossed the mitral vena contracta, but remained in the LV at the end of systole (Fig. 2a, b).

In order to identify the other, non-inflow components of the LV volume at end diastole, 400 particle traces were emitted from the LVOT during systole. Integration was performed backwards in time to demonstrate where the traces had come from; extraneous traces were removed by requiring crossing of an upstream LVOT plane. The remaining traces were then divided into Direct flow, which originated from the left atrium during the preceding diastole, and *Delayed Ejection flow,* which originated in the LV itself (Fig. 2c).

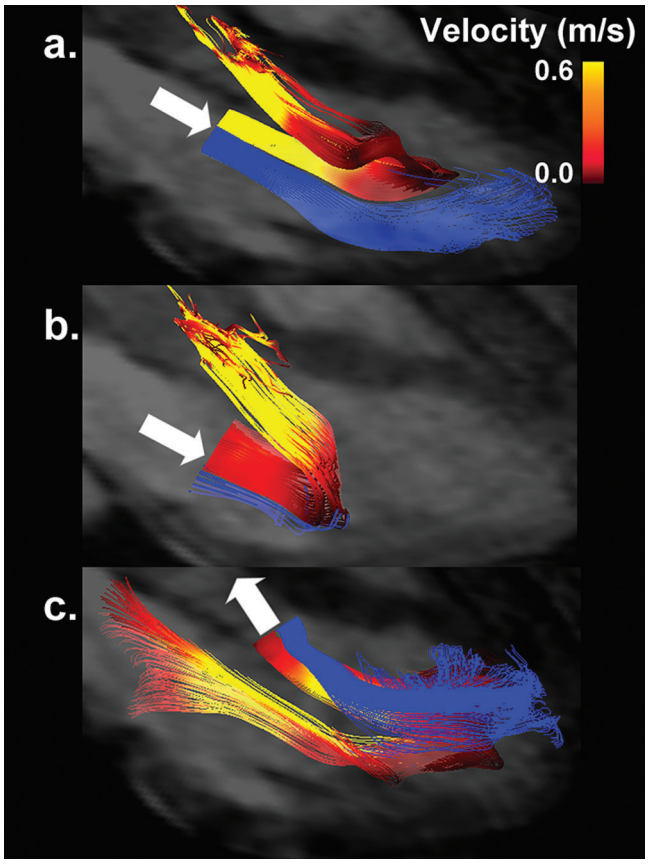

Figure 2. Components of left ventricular volume can be identified by their behavior. (**a**) Direct flow and Retained inflow traces are shown for early diastole. The arrow demonstrates the direction of flow. (**b**) Direct flow and Retained inflow traces are shown for late diastole (also see Videos 1 and 2). (**c**) Direct flow and Delayed Ejection outflow traces are emitted in early systole from the left ventricular outflow tract and traced backwards in time. Direct flow traces = velocity-encoded, red to yellow; Retained inflow and Delayed Ejection traces = blue.

Quantification of flow

Relative volumes of flow components

Every particle trace originated from an equal-sized patch of the original emitting grid. The flow volume represented by each trace was the product of the cross sectional area of its patch on the grid, its center velocity at the time of trace emission, and the duration of one time step. The inflow volume for each time step was the sum of volumes calculated for all inflow-generating patches. The total diastolic inflow volume was the sum of inflow volumes from all diastolic time steps and was separated into Direct and Retained inflow volumes. The volume of the Delayed Ejection flow was the sum of volumes from corresponding LVOT patches at all systolic time steps.

We anticipated that a final component of the total LVEDV would be a *Residual Volume* that had entered the LV more than one cycle before the analyzed beat and was destined to remain in the LV even after the next systole. This could not be visualized using particle trace methods. In order to obtain a rough estimate of the LV end-diastolic shape and volume, we created a wire frame hull (25) from the end-diastolic positions of all inflow and Delayed Ejection particle traces (Fig. 5a, d); its volume was taken as the estimated LV end diastolic volume (eLVEDV), and this enabled calculation of the Residual volume as:

$$\begin{aligned} \textit{Residual Volume} = \textit{eLVEDV} - (&\textit{Direct Flow} \\ &+ \textit{Retained Inflow} \\ &+ \textit{Delayed Ejection Flow}) \end{aligned} \quad [1]$$

Path length and energy

The path length of each particle trace was calculated from the sum of distances traveled between points of interest. The volume occupied by each trace could be combined with its velocity information to calculate instantaneous parameters of acceleration, deceleration and KE change. In order to calculate the total value for these parameters during the traces' diastolic transit through

the LV, integration began when the traces passed the mitral vena contracta plane, and ended when the particle trace either crossed the LVOT plane or at the end of diastole, whichever came first.

The kinetic energy, *KE*, of one particle trace was calculated as:

$$KE = m\frac{v^2}{2}, \qquad [2]$$

where $\boldsymbol{v}$ is the instantaneous velocity and m is the mass calculated from the density of blood times the trace's volume, measured at the time of emission as defined above. Change of inflowing kinetic energy during diastole for one particle trace was calculated as:

$$\Delta KE = m\frac{v_e^2 - v_s^2}{2}, \qquad [3]$$

where v_s and v_e are the velocities at the starting and ending points of interest.

Statistical analysis

The instantaneous, mean and integrated values of the measured parameters were calculated for each flow subsets' traces and expressed as a population average with standard deviation. The differences between flow subsets were compared using a Student's t test for paired observations; significance was assigned to a p value of <0.05.

RESULTS

Components of LV flow

The total inflow volume was 62 ± 9 mL, of which 44 ± 11% was Direct. The eLVEDV was 130 ± 20 mL. Direct flow, Retained Inflow, Delayed Ejection flow and Residual volume represented 21 ± 6, 27 ± 8, 27 ± 6 and 24 ± 1 percent of the eLVEDV, respectively (Fig. 3a). The origins, proportions and routes of the inflow components varied with the phase in the cardiac cycle (Figs. 2 and 4). Vortical flow was observed on the ventricular side of the mitral leaflets and in the LV apex in all subjects during diastole.

The path of the Direct flow through the LV was surrounded by a combination of anatomical and flow structures (Fig. 5b). Direct flow consistently occupied the basal half of the LV, swinging

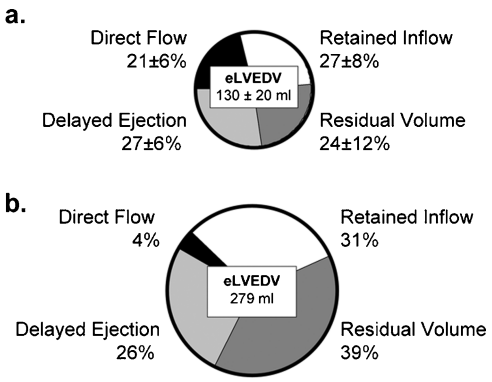

Figure 3. Relative proportions of the components of the end diastolic left ventricular blood volume (LVEDV). End-diastolic components in normal subjects (**a**) and in the myopathic left ventricle (**b**) are shown.

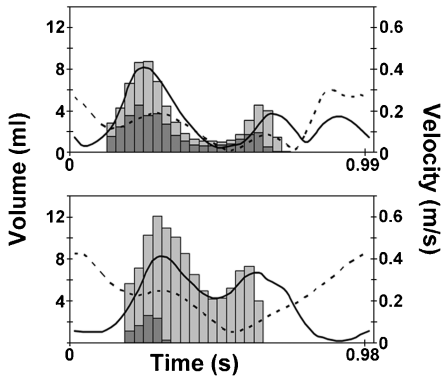

Figure 4. The timing and proportions of left ventricular inflow components vary with diastolic phase. Diastolic time steps are shown within a complete cardiac cycle. (**Upper panel**) A 50 y/o normal subject with heart rate 60 bpm. (**Lower panel**) A 51 y/o DCM patient with heart rate 62 bpm. E, peak early diastole; A, atrial contraction; mitral inflow velocity (–); pulmonary vein inflow velocity (- -); total inflow volume (light gray); Direct flow volume (dark gray).

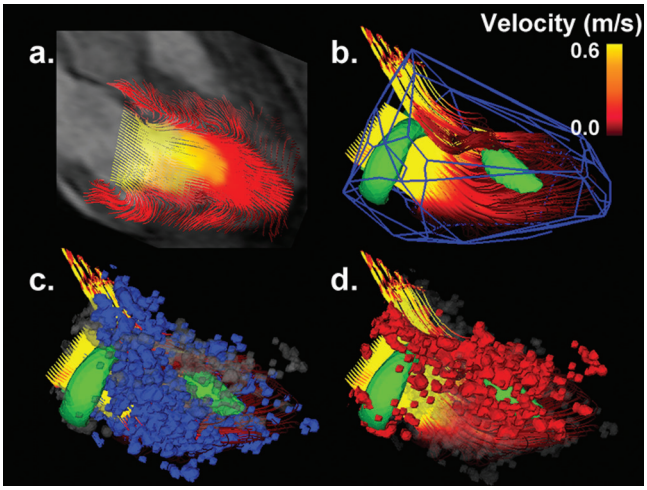

Figure 5. Normal LV diastolic flow. (**a**) Particle trace pathlines of short duration are emitted from a rectangular plane positioned along the LV long axis in early diastole (velocity-encoded, red to yellow). (**b**)The LV diastolic components include Direct inflow (velocity-encoded pathlines, red to yellow) and vortices (green vortex cores) near the mitral valve and in the apical region. (**c and d**) The end-diastolic positions of the particle traces are shown (dots). Retained inflow traces (blue dots) are distributed throughout the LV, with relative clustering in the posterolateral and subaortic regions of the LV. Delayed Ejection outflow (red dots) are distributed throughout the LV, with clustering in the septal-medial LV region.

Table 2. Left Ventricular Blood Flow Components and Characteristics

				Direct Inflow		Retained Inflow	
	Subject	eLVEDV (ml)	Percent of Inflow	Path Length (cm)	Change in Diastolic Kinetic Energy (mJ)	Path Length (cm)	Change in Diastolic Kinetic Energy (mJ)
Normals:	1	120	47.2	9.8	1.3	18.7	7.6
	2	154	23.3	8.3	0.6	13.6	6.9
	3	117	44.4	8.2	0.6	17.2	9.6
	4	129	26.4	7.2	0.9	12.4	7.5
	5	135	45.7	8.9	2.3	15.5	11.5
	6	179	47.5	8.1	2.3	17.1	9.0
	7	128	59.5	8.5	0.9	15.3	8.1
	8	161	64.8	9.1	3.1	18.9	8.1
	9	146	44.5	8.5	3.2	17.0	8.9
	10	118	36.6	7.5	0.7	11.9	4.9
	11	140	38.5	6.2	0.7	14.1	7.4
	12	109	37.3	9.1	0.7	14.1	8.7
	13	128	61.0	8.8	2.8	15.3	5.4
	14	115	47.6	7.0	1.1	11.1	6.5
	15	123	49.3	6.6	2.6	14.1	9.2
	16	116	47.7	5.5	2.7	11.3	8.0
	17	100	30.6	11.2	1.6	16.8	12.6
Patient:	DCM	279	11	13	0.6	16	11
Normals:	Average ± SD:	130.4 ± 20.2	44.2 ± 11.4	8.1 ± 1.4	1.6 ± 1.0	15.0 ± 2.4*	8.2 ± 1.9*
	Range:	99.6 – 178.9	23.2 – 64.8	5.5 – 11.2	0.6 – 3.2	11.1 – 18.9	4.9 – 12.6

eLVEDV = end-diastolic volume estimated with particle trace end points, DCM = dilated cardiomyopathy, mJ = millijoules, SD = standard deviation. *$p < 0.05$ compared to Direct inflow.

around the edge of the anterior leaflet and its corresponding vortex before turning smoothly towards the LV outflow tract. Other flow components were clustered in other LV regions (Fig. 5c, d).

The average path length of Direct flow from the mitral vena contracta to the LV outflow tract was 8 ± 1 cm; path lengths became progressively shorter during diastole. The path length of the Retained inflow was 15 ± 2 cm, assuming a single additional cycle before ejection.

LV inflow kinetic energy

Inflow that followed the Direct route retained more of its KE through the course of diastole than Retained inflow (1.6 ± 1.0 millijoules vs 8.2 ± 1.9 millijoules, Table 2). Retained inflow accounted for 84% of the total diastolic reduction of the inflow KE.

Cardiomyopathic LV flow

A single subject with dilated cardiomyopathy (DCM) was included for preliminary comparison to the normal subjects (Fig. 6). The LV was mildly dilated and its systolic function was moderately depressed (end-diastolic internal diameter and LVEF by echocardiography, 6.1 cm and 31% respectively). The eLVEDV was approximately twice that of normals. The route of Direct flow in the dilated LV was similar to normals (Fig. 6 b), but only 11% of the total LV inflow was Direct (Table 2). Direct flow came from only the first 30% of diastole, in marked

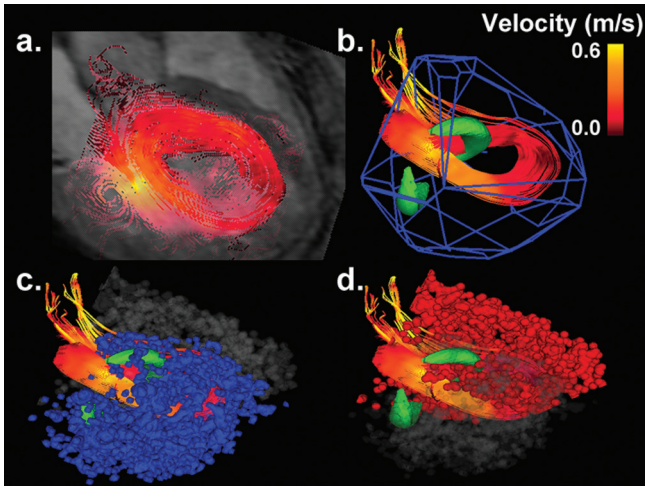

Figure 6. LV diastolic flow in a patient with DCM. (**a**) Particle trace pathlines of short duration are emitted from a rectangular plane positioned along the LV long axis in a cardiomyopathic subject in early diastole (velocity-encoded, red to yellow). (**b**)The LV diastolic components include Direct inflow (velocity-encoded pathlines, red to yellow) and vortices indicated by the green vortex cores near the mitral valve and in the apical region (also see Video 3). (**c and d**) The end-diastolic positions of the particle traces are shown (dots). Retained inflow traces (blue dots) are clustered in the posterolateral LV, and the Delayed Ejection outflow (red dots) are clustered in the septal-medial LV region.

contrast to the normal subjects (Fig. 4). On a per mL basis, in DCM the Direct flow diastolic KE losses were comparable to normal subjects (0.07 versus 0.06 ± 0.03 millijoules/mL); because of the small amount of Direct flow in the DCM subjection, however, only 5% of the total inflow diastolic KE was preserved (compared to 16 ± 8% in normal subjects). Extensive flow recirculation was seen (Fig. 6a, Video 3); the KE loss of Retained inflow was 18-fold greater than Direct flow.

DISCUSSION

Phase contrast CMR provides three dimensional, three directional, time resolved velocity data which allow the visualization of complex intracavitary flow, in contrast to imaging methods where flow "disappears" as it turns out of a plane or out of alignment with an ultrasound beam. Inherently multidimensional flow imaging tools allow us to address important questions about normal blood flow patterns, and the impact of cardiovascular disease on them. Animations of particle trace pathlines demonstrate the interplay of flow components (videos 1 and 2), and this approach also permits subsequent quantification of flow components.

Compartmentalization of ventricular flow has been proposed previously: mixing within the beating LV has been estimated at less than 15% (26). Similar observations have been made in the right ventricle (27). Although effectively averaged over many heartbeats, the results of this study are in accord with the notion of distinct behaviors of LV blood flow components, and the components' relative volumes and changes of KE during diastole are estimated here for the first time.

Direct and retained flow through the LV

The relatively short course of the direct path in and out of the LV conserves more of its KE through diastole, which may be a mark of fluid dynamic efficiency. Loss of KE does not necessarily imply dissipation of energy, however, as some may be transferred to elastic potential energy in the myocardium and elsewhere. Of interest, the direct route appears to be shaped as much by concurrent flows as by familiar anatomic structures. The degree to which the heart is able to utilize this pathway may depend on the other subsets of the ventricular volume and how they are distributed in the setting of myocardial dysfunction, chamber dilation or arrhythmia.

Direct flow entering the LV in late diastole seems to show the least change of speed and traces the shortest distance from inflow to ejection. Atrial contraction also impacts other flow components, increasing the rotational speed of the mitral vortices and accelerating flow towards the LVOT. This "boost" in late diastolic velocity may preserve diastolic momentum (28). These properties may be more marked in the exercising state, which was not studied.

The Retained portion of LV inflow spends more than a single beat within the heart. Our data suggest that most of this volume becomes the Delayed Ejection volume for the subsequent beat, and that the normal LV achieves effective volume exchange over very few beats. Extensive recirculation of LV volume in the setting of DCM has been reported (29); multidimensional flow mapping in the DCM subject suggests that only a small portion of the most peripheral recirculation volume is ejected (video 3). The diversion of inflow KE and systolic myocardial work to flow rotation rather than to ejection may contribute to the inefficiency of DCM.

Limitations

This particle trace method is sensitive to noise and systematic errors along the pathline. Respiratory compensation was not applied in acquiring these data, which may cause blurring of small flow structures and at the edges of the cavity. In addition, acceleration of flow may lead to errors in estimation of peak velocities (30); this would be more relevant to systolic than to diastolic events. Another limitation is that the spatial and temporal averaging used here will obscure minor flow disturbances or instabilities as well as the mixing of concurrent streams.

LVEDV measurement based on endocardial segmentation would have been optimal; these phase contrast data provided inadequate anatomical outline to allow this. The wire frame depiction and estimation of the LVEDV based on particle traces were performed to provide a context for flow visualization, despite its expected limitations. The true endocardial border cannot be identified because the traces become unreliable at very low velocities. The density of the traces, the distribution of the residual volume, and the accuracy of the particle trance integration will also affect the eLVEDV representation.

Conclusions

Particle trace methods create dynamic multidimensional images of flow that allow quantification of the volume, distribution, timing and of diastolic KE changes of separate components of intraventricular flow. Compartmentalization of flow and an efficient direct route through the diastolic LV may be basic aspects of normal cardiac physiology; they may reflect changes in LV configuration, myocardial function and pressure distribution that occur with disease. Future improvements in spatial and temporal resolution will make this particle trace approach more accurate; analysis of subjects across a range of heart rates and ages will be necessary to evaluate these preliminary findings in a broader spectrum of normal individuals as well as patients. Lessons from this type of multidirectional flow mapping may be relevant to the design of valvular prostheses, surgical and pacing strategies, and the individualization of therapy (31–36).

ABBREVIATIONS

3D = three dimensional
LV = left ventricle
VC = vena contracta
mJ = millijoules
ml = milliliters
LVEDV = left ventricular end-diastolic volume
eLVEDV = estimated left ventricular end-diastolic volume from particle trace method

ROI = region-of-interest
LVOT = left ventricular outflow tract
KE = kinetic energy

REFERENCES

1. Bellhouse BJ, Bellhouse FH. Fluid mechanics of the mitral valve. Nature 1969;224:615–16.
2. McQueen DM, Peskin CS, Yellin EL. Fluid dynamics of the mitral valve: physiological aspects of a mathematical model. Am J Physiol 1982;242:H1095–1110.
3. Saber NR, Gosman AD, Wood NB, Kilner PJ, Charrier CL, Firmin DN. Computational flow modeling of the left ventricle based on in vivo MRI data: initial experience. Ann Biomed Eng 2001;29:275–83.
4. Cheng Y, Oertel H, Schenkel T. Fluid-structure coupled CFD simulation of the left ventricular flow during filling phase. Ann Biomed Eng 2005;33:567–76.
5. Courtois M, Barzilai B, Gutierrez F, Ludbrook PA. Characterization of regional diastolic pressure gradients in the right ventricle. Circulation 1990;82:413–23.
6. Saber NR, Wood NB, Gosman AD, Merrifield RD, Yang GZ, Charrier CL, Gatehouse PD, Firmin DN. Progress towards patient-specific computational flow modeling of the left heart via combination of magnetic resonance imaging with computational fluid dynamics. Ann Biomed Eng 2003;31:42–52.
7. Pasipoularides A, Shu M, Shah A, Tucconi A, Glower DD. RV instantaneous intraventricular diastolic pressure and velocity distributions in normal and volume overload awake dog disease models. Am J Physiol Heart Circ Physiol 2003;285:H1956–65.
8. Kim WY, Walker PG, Pedersen EM, Poulsen JK, Oyre S, Houlind K, Yoganathan AP. Left ventricular blood flow patterns in normal subjects: a quantitative analysis by three-dimensional magnetic resonance velocity mapping. J Am Coll Cardiol 1995;26:224–38.
9. Walker PG, Cranney GB, Grimes RY, Delatore J, Rectenwald J, Pohost GM. Three-dimensional reconstruction of the flow in a human left heart by using magnetic resonance phase velocity encoding. Ann Biomed Eng 1996;24:139–47.
10. Yang GZ, Mohiaddin RH, Kilner PJ, Firmin DN. Vortical flow feature recognition: a topological study of in vivo flow patterns using MR velocity mapping. J Comput Assist Tomogr 1998;22:577–86.
11. Thanigaraj S, Chugh R, Schechtman KB, Lee LV, Wade RL, Perez JE. Defining left ventricular segmental and global function by echocardiographic intraventricular contrast flow patterns. Am J Cardiol 2000;85:65–68.
12. Kilner PJ, Yang GZ, Wilkes AJ, Mohiaddin RH, Firmin DN, Yacoub MH. Asymmetric redirection of flow through the heart. Nature 2000;404:759–61.
13. Fyrenius A, Wigstrom L, Ebbers T, Karlsson M, Engvall J, Bolger AF. Three dimensional flow in the human left atrium. Heart 2001;86:448–55.
14. Ebbers T, Wigström L, Bolger AF, Wranne B, Karlsson M. Noninvasive measurement of time-varying three-dimensional relative pressure fields within the human heart. J Biomech Eng 2002;24:288–93.
15. Beppu S, Izumi S, Miyatake K, Nagata S, Park YD, Sakakibara H, Nimura Y. Abnormal blood pathways in left ventricular cavity in acute myocardial infarction: Experimental observations with special reference to regional wall motion abnormality and hemostasis. Circulation 1988;78:157–64.
16. Jacobs LE, Kotler MN, Parry WR. Flow patterns in dilated cardiomyopathy: a pulsed-wave and color flow Doppler study. J Am Soc Echocardiogr 1990;3:294–302.
17. Houlind K, Schroeder AP, Stodkilde-Jorgensen H, Paulsen PK, Egeblad H, Pedersen EM. Intraventricular dispersion and temporal delay of early left ventricular filling after acute myocardial infarction. Assessment by magnetic resonance velocity mapping. Magn Reson Imaging 2002;20:249–60.
18. Wigström L, Sjöqvist L, Wranne B. Temporally resolved 3D phase contrast imaging. Magn Reson Med 1996;36:800–3.
19. Xiang QS. Temporal phase unwrapping for CINE velocity imaging. J Magn Reson Imaging 1995;5:529–34.
20. Wigström L, Ebbers T, Fyrenius A, Karlsson M, Engvall J, Wranne B, Bolger AF. Particle trace visualization of intracardiac flow using time resolved 3D phase contrast MRI. Magn Reson Med 1999;41:793–99.
21. Bernstein MA, Zhou XJ, Polzin JA, King KF, Ganin A, Pelc NJ, Glover GH. Concomitant gradient terms in phase contrast MR: analysis and correction. Magn Reson Med 1998;39:300–8.
22. Heiberg E, Ebbers T, Wigström L, Karlsson M. Three dimensional flow characterization using vector pattern matching. IEEE Transactions on Visualization and Computer Graphics 2003;9:313–19.
23. Darmofal D, Haimes R. An analysis of 3D particle path integration algorithms. Journal of Computational Physics 1996;123:182–95.
24. Buonocore MH. Visualizing blood flow patterns using streamlines, arrows, and particle paths. Magn Reson Med 1998;40:210–26.
25. Barber CB, Dobkin DP, Huhdanpaa HT. The quickhull algorithm for convex hulls. ACM Transactions on Mathematical Software 1996;22:469–83.
26. Irisawa H, Wilson MF, Rushmer RF. Left ventricle as a mixing chamber. Circ Res 1960;8:183–87.
27. Globits S, Pacher R, Frank H, Pacher B, Mayr H, Neuhold A, Glogar D. Comparative assessment of right ventricular volumes and ejection fraction by thermodilution and magnetic resonance imaging in dilated cardiomyopathy. Cardiology 1995;86:67–72.
28. Noble MI. The contribution of blood momentum to left ventricular ejection in the dog. Circ Res 1968;23:663–70.
29. Mohiaddin RH. Flow patterns in the dilated ischemic left ventricle studied by MR imaging with velocity vector mapping. J Magn Reson Imaging 1995;5:493–98.
30. Thunberg P, Wigstrom L, Wranne B, Engvall J, Karlsson M. Correction for acceleration-induced displacement artifacts in phase contrast imaging. Magn Reson Med 2000;43:734–38.
31. Taylor CA, Draney MT, Ku JP, Parker D, Steele BN, Wang K, Zarins CK. Predictive medicine: computational techniques in therapeutic decision-making. Comput Aided Surg 1999;4:231–47.
32. Yacoub MH, Kilner PJ, Birks EJ, Misfeld M. The aortic outflow and root: a tale of dynamism and crosstalk. Ann Thorac Surg 1999;68:S37–43.
33. Kozerke S, Hasenkam JM, Pedersen EM, Boesiger P. Visualization of flow patterns distal to aortic valve prostheses in humans using a fast approach for cine 3D velocity mapping. J Magn Reson Imaging 2001;13:690–98.
34. Kvitting JPE, Ebbers T, Wigstrom L, Engvall J, Olin CL, Bolger AF. Flow patterns in the aortic root and the aorta studied with time-resolved, 3-dimensional, phase-contrast magnetic resonance imaging: implications for aortic valve-sparing surgery. J Thorac Cardiovasc Surg 2004;127:1602–7.
35. Machler H, Perthel M, Reiter G, Reiter U, Zink M, Bergmann P, Waltensdorfer A, Laas J. Influence of bileaflet prosthetic mitral valve orientation on left ventricular flow-an experimental in vivo magnetic resonance imaging study. Eur J Cardiothorac Surg 2004;26:747–53.
36. Markl M, Draney MT, Miller DC, Levin JM, Williamson EE, Pelc NJ, Liang DH, Herfkens RJ. Time-resolved three-dimensional magnetic resonance velocity mapping of aortic flow in healthy volunteers and patients after valve-sparing aortic root replacement. J Thorac Cardiovasc Surg 2005;130:456–63.